




## Impact of sodium nitroprusside concentration added to batch cultures of *Escherichia coli* biofilms on the c-di-GMP levels, morphologies and adhesion of biofilm-dispersed cells

Ayse Ordek & F. Pinar Gordesli-Duatepe


To cite this article: Ayse Ordek & F. Pinar Gordesli-Duatepe (2022) Impact of sodium nitroprusside concentration added to batch cultures of *Escherichia coli* biofilms on the c-di-GMP levels, morphologies and adhesion of biofilm-dispersed cells, *Biofouling*, 38:8, 796-813, DOI: [10.1080/08927014.2022.2131399](https://doi.org/10.1080/08927014.2022.2131399)



To link to this article: <https://doi.org/10.1080/08927014.2022.2131399>

 View supplementary material 

 Published online: 13 Oct 2022.

 Submit your article to this journal 

 Article views: 230

 View related articles 

 View Crossmark data 



## Impact of sodium nitroprusside concentration added to batch cultures of *Escherichia coli* biofilms on the c-di-GMP levels, morphologies and adhesion of biofilm-dispersed cells

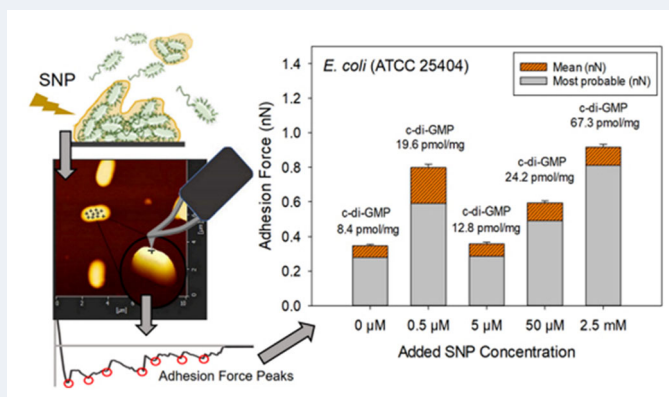
Ayse Ordek<sup>a</sup>  and F. Pinar Gordesli-Duatepe<sup>b</sup> 

<sup>a</sup>Bioengineering Graduate Program, Graduate School, Izmir University of Economics, Izmir, Turkey; <sup>b</sup>Department of Genetics and Bioengineering, Faculty of Engineering, Izmir University of Economics, Izmir, Turkey

### ABSTRACT

Biofilm dispersion can be triggered by the application of dispersing agents such as nitric oxide (NO)-donors, resulting in the release of biofilm-dispersed cells into the environment. In this work, biofilm-dispersed cells were obtained by adding different concentrations of NO-donor sodium nitroprusside (0.5, 5, 50  $\mu$ M, and 2.5 mM of SNP) to batch cultures of pre-formed *Escherichia coli* biofilms. Except for those dispersed by 5  $\mu$ M of SNP, biofilm-dispersed cells were found to be wider and longer than the planktonic cells and to have higher c-di-GMP levels and greater adhesion forces to silicon nitride surfaces in water as measured by atomic force microscope. Consequently, the optimum concentration of SNP to disperse *E. coli* biofilms was found to be 5  $\mu$ M of SNP, whose addition to batch cultures resulted in a significant biofilm dispersion and the dispersed cells having c-di-GMP levels, morphologies and adhesion strengths similar to their planktonic counterparts.

### GRAPHICAL ABSTRACT



### ARTICLE HISTORY

Received 1 April 2022  
Accepted 28 September 2022  
Published Online 13 October 2022

### KEYWORDS


Biofilm-dispersed cells; *Escherichia coli*; sodium nitroprusside (SNP); c-di-GMP; adhesion force; atomic force microscope (AFM)

## Introduction

Bacterial cells can exist in the form of a planktonic-motile single-cell state, or the form of communities of complex architectures surrounded by an extracellular polymeric matrix at a liquid-solid interface, in other words as biofilms (Donlan 2002; Hall-Stoodley *et al.* 2004). Many bacteria can attach to and colonise surfaces by forming a biofilm, allowing them to persist in the environment and resist harsh conditions including

treatments with antimicrobials and disinfectants (Davies 2003; Bridier *et al.* 2011). Biofilms are the major source of biofouling in industrial water systems as they cause damage to the equipment and materials, and losses in production (Donlan 2002; Galié *et al.* 2018). Biofilms formed on the surfaces of processing equipment in contact with food are the sources of contamination that threaten the quality and safety of food products (Galié *et al.* 2018) and hence human health. In hospital settings, biofilms have been shown

CONTACT F. Pinar Gordesli-Duatepe  [pinar.gordesli@iue.edu.tr](mailto:pinar.gordesli@iue.edu.tr)

 Supplemental data for this article can be accessed online at <https://doi.org/10.1080/08927014.2022.2131399>

This article has been republished with minor changes. These changes do not impact the academic content of the article.

© 2022 Informa UK Limited, trading as Taylor & Francis Group

to persist on various medical devices and patients' tissues, causing persistent infections (Percival *et al.* 2015). As a result of their persistence and chronic nature, biofilms are estimated to be responsible for 65–80% of microbial and chronic infections occurring in the human body (Davies 2003; Chua *et al.* 2014). Biofilms are of great public health concern due to their resistance to antibiotics, which is approximately 10–1000 times higher than the planktonic cells, and their abilities to tolerate host defence systems and other external stresses (Mah 2012; Sharma *et al.* 2019).

Biofilm formation is usually established through a developmental process with different stages (Koo *et al.* 2017). First, planktonic cells attach to the surface through their cell surface-associated biopolymers. After the initial adhesion to the surface, bacterial cells begin to divide and produce extracellular polymeric substances (EPS). Later in the maturation stage, the biofilm transforms into a structured architecture with the help of EPS, which provides a multifunctional and protective scaffold. After maturation, some bacterial cells leave the biofilm to explore other niches and attach to a new surface, which is the final stage of the biofilm life cycle, known as the dispersion stage (Chua *et al.* 2014; Koo *et al.* 2017). Biofilm dispersion can be triggered by the application of dispersing agents such as quorum-sensing compounds/inhibitors (QSI), heavy metals, and nitric oxide (NO)-donors. However, it can be challenging to apply QSI and heavy metals because the EPS matrix can bind to and sequester QSI during their diffusion process (Koo *et al.* 2017), and the applicability of heavy metals in healthcare is questionable due to their high toxicity (Wille and Coenye 2020). On the other hand, triggering of biofilm dispersion by the application of NO-donors has been proposed as a promising strategy for the removal of biofilms from surfaces (Barraud *et al.* 2006; 2009a, 2009b; Werwinski *et al.* 2011; Barnes *et al.* 2013; Howlin *et al.* 2017). However, the NO-donors to be applied should be safe, stable, and environmentally friendly. In this context, NO-donor sodium nitroprusside (SNP), used as an FDA-approved drug in the treatment of hypertension, has the advantage of releasing steady-state levels of NO that mimic endogenous NO production. While other NO-donors such as 3-(aminopropyl)-1-hydroxy-3-isopropyl-2-oxo-1-triazene (NOC-5) and propylamine propylamine NONOate (PAPA-NONOate) degrade substantially within days, SNP has been shown to have great stability releasing consistent NO levels over days (Bradley and Steinert 2015). Moreover, SNP has

been shown to induce the dispersion of pre-formed *Pseudomonas aeruginosa* biofilm colonies *in vitro* and increases the effectiveness of antibiotics in the removal of biofilms (Barraud *et al.* 2006). Given the long history of clinical use of SNP as an FDA-approved drug, no serious health or environmental risks are expected from its application at low concentrations.

Studies investigating the mechanisms of NO-induced biofilm dispersion in *P. aeruginosa* have revealed that NO signalling is a part of the global regulatory network that controls the transition from biofilm to planktonic form and involves the intracellular secondary messenger nucleotide, cyclic diguanylate monophosphate (c-di-GMP) (Barraud *et al.* 2006; 2009a; Chua *et al.* 2014). The biofilm dispersal effect of SNP was suggested to be due to the release of NO, which was shown to regulate c-di-GMP levels and mediate *P. aeruginosa* biofilm dispersion when applied at low concentrations (Barraud *et al.* 2006; Chua *et al.* 2014). The dispersal effect of low dose SNP (in the micromolar range) has been reported not only for *P. aeruginosa* biofilms (Barraud *et al.* 2006; Barnes *et al.* 2013) but also for biofilms formed by other bacterial species such as *Escherichia coli*, *Vibrio cholera*, *Staphylococcus epidermidis*, *Bacillus licheniformis* (Barraud *et al.* 2009b) and *Pseudoalteromonas* sp (Werwinski *et al.* 2011). However, these studies often did not investigate the initial adhesion of freshly dispersed cells to surfaces, the first stage in the biofilm formation process, compared to those of their planktonic counterparts or did not test the effect of different concentrations of SNP on the adhesive properties of biofilm-dispersed cells. This is partly because cells dispersed from biofilms have been assumed to immediately go into the planktonic growth phase. However, Chua *et al.* (2014) showed that the physiology of cells dispersed from *P. aeruginosa* biofilms (either by applying 5  $\mu$ M of SNP or by inducing the expression of a plasmid-encoded YhjH phosphodiesterase) is fairly different from that of planktonic and biofilm cells. Dispersed cells were also found to be highly virulent against macrophages and *Caenorhabditis elegans* compared to planktonic cells. Since dispersed cells represent a different intermediate step between planktonic and biofilm forms of existence, and as biofilm dispersion can be the beginning of a new life cycle, it has become extremely important to investigate not only the biochemical and biophysical properties but also the nanoscale adhesion characteristics of dispersed cells relative to those of their planktonic counterparts. In addition, given that the dispersed cell

phenotype was maintained in the presence of dispersing agents (Chua *et al.* 2014), it is significant to investigate the effect of the concentration of the dispersing agent used on such characteristics to develop improved strategies to combat biofilms.

In this study, the c-di-GMP levels, morphologies, and adhesion characteristics of planktonic and biofilm-dispersed *E. coli* cells were compared as functions of SNP concentrations added to batch cultures of *E. coli* biofilms. Planktonic *E. coli* cells were obtained by growing the cells until the late exponential phase, as this phase is linked to the highly motile planktonic bacterial lifestyle (Pesavento *et al.* 2008; Povolotsky and Hengge 2012). Since the transition between different bacterial lifestyles can be seen more clearly in a batch culture due to the homogeneity observed in the physiological state of bacterial cells (Povolotsky and Hengge 2012), biofilm-dispersed cells were obtained by adding different concentrations of SNP (0.5, 5, 50  $\mu$ M, and 2.5 mM) to batch cultures of pre-formed *E. coli* biofilms. Intracellular c-di-GMP levels of the cells were determined by the traditional high-performance liquid chromatography (HPLC) technique. The morphologies and adhesion characteristics of the cells were determined by an atomic force microscope (AFM). AFM offers an ideal platform for evaluating the nanoscale adhesion forces between two surfaces that are in contact with each other (Dufre ne 2015; Alsteens *et al.* 2017). AFM also provides quantitative information on the morphology of bacterial cells (Soon *et al.* 2009; Bashiri *et al.* 2021), and the heterogeneity (Dorobantu *et al.* 2008; Ma *et al.* 2008; Park and Abu-Lail 2011; El-Kirat-Chatel *et al.* 2017), adhesion strength (Abu-Lail and Camesano 2003; Gordesli and Abu-Lail 2012a, 2012b, Ramezani *et al.* 2018), structure and mechanics (Park and Abu-Lail 2010; Gordesli and Abu-Lail 2012c; Auer and Weibel 2017) of bacterial surface biopolymers under room conditions or in the presence of liquid media in real-time. Here, AFM was utilized to determine the dimensions (height, width, and length) of planktonic and biofilm-dispersed *E. coli* cells, the heterogeneities and the lengths (pull-off distances) of bacterial surface biopolymers and their nanoscale adhesion forces to silicon nitride surfaces in water.

## Materials and methods

### Bacterial strain and culture conditions for planktonic growth

*Escherichia coli* thrives in freshwater, marine water, soil, and the mammalian gut, and forms biofilms

under different abiotic and biotic stresses (Povolotsky and Hengge 2012). *E. coli* K-12 wild-type strain ATCC 25404 was chosen as the model bacterial strain because it was shown to form mature biofilms displaying higher biomass compared to other *E. coli* strains such as MG1655, BW25113 or JM109 (Wood *et al.* 2006). *E. coli* ATCC 25404 cells were grown overnight for 12-h in Luria-Bertani broth (LB) at 30 °C in a temperature-controlled shaker rotating at 170 rpm. Then, 1% (v/v) of the bacterial culture was transferred into a fresh medium and incubated at 37 °C, 170 rpm. The growth of the bacterial cells was monitored by reading the optical density of the culture against time at a wavelength of 600 nm using the UV/visible spectrophotometer. After 4-h of incubation, cells that reached a late exponential phase of growth were centrifuged three times at 3000 rpm and harvested as planktonic cells for use in further investigation.

### Procedure for obtaining biofilm-dispersed cells from batch cultures

*Escherichia coli* cells were grown overnight in LB for 12-h. The culture was then diluted in fresh LB (corresponding to  $1.0 \times 10^7$  CFU/ml) and transferred into sterile polystyrene 96-well microplates (Corning 3788, non-treated) for biofilm assays. After 17-h of incubation at 37 °C, media containing unattached cells that did not contribute to the formation of biofilms was carefully removed by washing the wells twice with deionized (DI) water (Merritt *et al.* 2005; O'Toole 2011). For dispersion assays, fresh LB medium containing 15 different concentrations of SNP (0.125  $\mu$ M up to 100 mM of SNP) was added into the wells (for the control group, only fresh LB medium was added), and incubated at 37 °C for 24-h with shaking at 120 rpm. After 24-h of incubation in SNP-added media, bacterial cultures in the microplates were transferred into new polystyrene 96-well microplates. Then the optical densities of the cultures were measured at 600 nm (OD600 nm). Biofilm dispersion experiments were performed independently three times, and 24 replicate wells per SNP treatment were used in each experiment. Only the cells dispersed by the addition of 0.5, 5, 50  $\mu$ M and 2.5 mM of SNP were collected from the wells for further investigation.

### Quantification of remaining biofilms

For quantification of biofilms (control group and remaining biofilms after SNP-induced dispersal) in 96-well microplates, the basic protocol given as

microtiter plate biofilm assay (O'Toole 2011) was followed. Biofilms formed in wells filled with fresh LB without the addition of SNP were the control group. First, microplates containing the biofilms were washed twice with DI water. Then, a 0.1% solution of crystal violet (CV) in water was added to each well of the microplates. The plates were incubated at room temperature for 10–15 min. After staining the biofilms with CV, the wells were washed three times with DI water and allowed to air-dry. To solubilize the CV, 200  $\mu$ l of 30% acetic acid solution in water was added to each well and incubated for 10–15 min. The absorbance of CV was quantified for each well at 595 nm (CV595 nm) using an ELISA reader. Acetic acid (30%) in water was used as the blank.

### Quantification of biofilm indexes

For each SNP concentration investigated, the biofilm index was quantified as the ratio of CV staining of the biofilm measured at 595 nm (CV595 nm) to the optical density of the bacterial culture in the bulk-liquid in the same well measured at 600 nm (OD600 nm). The mean value of the biofilm index, defined as the fold increase/decrease in the biofilm biomass relative to bacterial biomass in the bulk-liquid, was used as an indicator of the biofilm dispersion. In addition, viable bacteria within the biofilms and the microplate wells were enumerated for those exposed to 0.5, 5, 50  $\mu$ M and 2.5 mM of SNP concentrations. Viable counts confirmed the dispersion of the biofilms (Figure S1).

### Extraction of *c*-di-GMP from planktonic and biofilm-dispersed bacterial cells

The *c*-di-GMP levels of planktonic and biofilm-dispersed *E. coli* cells were determined in terms of pmol *c*-di-GMP per mg of protein by adapting the protocol developed by Petrova and Sauer (2017). Briefly, to obtain the optical density of bacterial cultures from which detectable levels of *c*-di-GMP could be extracted, cells dispersed from biofilms by the addition of media containing 0.5, 5, 50  $\mu$ M, and 2.5 mM of SNP were transferred to fresh LB media containing the same concentrations of SNP, respectively, and grown for 4-h at 37 °C, 170 rpm. Planktonic cells were harvested at the late exponential phase of growth, as previously described. Subsequently, the optical densities of the bacterial cultures were adjusted to OD<sub>600</sub>  $\sim$  1.5 in 1 ml of respective culture volume. Bacterial cultures were then centrifuged at 16,000 *g* for 2 min at 4 °C.

After centrifugation, cell pellets were washed with 1 ml ice-cold PBS and centrifuged again. Supernatants were discarded and the washing step was repeated one more time. The remaining pellets were mixed with 100  $\mu$ l ice-cold PBS for each investigated and incubated at 100 °C for 5 min. After incubation, 217  $\mu$ l of ice-cold ethanol was added and vortexed. Samples were centrifuged (16,000 *g*, 2 min, 4 °C), cell pellets were retained, and the supernatants containing extracted *c*-di-GMP were transferred into new tubes. Using the cell pellets, the extraction step was repeated two more times. After the final extraction step, cell pellets were retained and stored at –20 °C for subsequent protein quantification. For each condition investigated, the supernatants from the repeated extractions were combined in one microfuge tube and freeze-dried. The whole extraction procedure was done independently three times for each condition investigated. The total protein content of the retained cell pellets was determined using a modified Lowry protein assay kit (Pierce, Rockford, IL). Bovine serum albumin (BSA) was used as the standard.

### Detection and quantification of extracted *c*-di-GMP from planktonic and biofilm-dispersed bacterial cells

Experiments were performed using Ultimate 3000 HPLC (Thermo Fisher Scientific, Waltham, MA) equipped with an autosampler, degasser, pump, and UV/Vis detector set to 253 nm. Separation was carried out using a reverse-phase C18 column (4.6  $\times$  100 mm, particle size 5  $\mu$ m, Thermo Fisher Scientific). The mobile phases used were 10 mM ammonium acetate (MS-grade) in ultrapure water (phase A) and 10 mM ammonium acetate (MS-grade) in methanol (phase B) (Petrova and Sauer 2017). The gradient program was initiated with a flow rate of 0.5 ml min<sup>–1</sup> using 1% B and 99% A for 0–9 min; 15% B and 85% A, 9–14 min; 25% B and 75% A, 14–19 min; 90% B and 10% A, 19–26 min; 1% B and 99% A for 26–45 min. Standard solutions of *c*-di-GMP (1, 5, 10 and 20 pmol/ $\mu$ l) were prepared from the authentic Bis-(3'–5')-cyclic diguanylic monophosphate (*c*-di-GMP) (Bio-log). Nanopure water was used as the negative control. 20  $\mu$ l of each standard solution was injected and run on HPLC, and the coincident chromatogram of *c*-di-GMP standards was created where the elution of *c*-di-GMP was observed at approximately  $\sim$  17.2 min (Figure S2). A calibration plot (standard curve) of *c*-di-GMP standards was generated by determining the peak area for each of the standard concentrations using Chromeleon™ 7.3 Chromatography Data

System (CDS) software (Figure S3). Before experiments, dried *c*-di-GMP extracts were resuspended in 300  $\mu$ L of nanopure water for each condition investigated and vortexed for 1 min. Then, suspensions were centrifuged at 16,000 g for 2 min to remove the insoluble contents. Supernatants containing *c*-di-GMP were filtered into vials using 0.22- $\mu$ m syringe filters. A volume of 20  $\mu$ L of each sample solution was injected into the HPLC system, and the concentration of *c*-di-GMP per sample was determined using the standard curve previously generated (Figure S3). Finally, the *c*-di-GMP levels were normalized to total cellular protein levels.

### Sample preparation for AFM measurements

AFM samples were prepared by adapting the protocols given by Wang *et al.* (2019). Briefly, 100  $\mu$ L of 0.01% (w/v) poly-L-lysine (PLL) solution was spread over the mica surface (approximately 1.5 cm<sup>2</sup> surface area). The solution was allowed to sit on the mica surface for about 2–3 h, while the disk remained closed inside a Petri dish. Then, the disk was thoroughly washed-off with DI water and allowed to dry for about 1-h at room temperature before cell immobilization. Planktonic cells and biofilm-dispersed cells obtained by the addition of 0.5, 5, 50  $\mu$ M and 2.5 mM of SNP (freshly collected as described above) were centrifuged three times at 3000 rpm for 5 min. After

centrifugation, 20  $\mu$ L aliquot of bacterial suspension was added on air-dried PLL-coated mica disc for each condition investigated and incubated for 10 min. After that, the disc was washed 3 times with DI water to remove the non-adhering bacteria and was ready for AFM measurements. Bacterial cells immobilized on PLL-coated mica surfaces were intact and possessed their typical rod shape morphology in DI water (Figure 1). In addition, overall cell viability was not significantly affected after immobilizing planktonic and biofilm-dispersed cells on PLL-coated mica surfaces (Figure S4). It should be noted that washing the bacteria with DI water may increase bacterial death through the change of osmotic pressure. If bacterial integrity and viability cannot be maintained, phosphate-buffered saline can be used instead of DI water.

### Atomic force microscopy (AFM) measurements

All AFM imaging and force measurements were carried out under DI water using silicon nitride cantilevers (DNP-S cantilevers with 0.24 N/m nominal spring constant, Bruker AXS Inc., Santa Barbara, CA). Silicon nitride cantilevers were chosen as our model inert surfaces because they are characterized by similar surface potentials to that of soil and glass (Abu-Lail and Camesano 2003), substrates to which bacterial cells frequently attach in nature (Borer *et al.* 2018). Before starting the scan, the vibration spectrum (Q

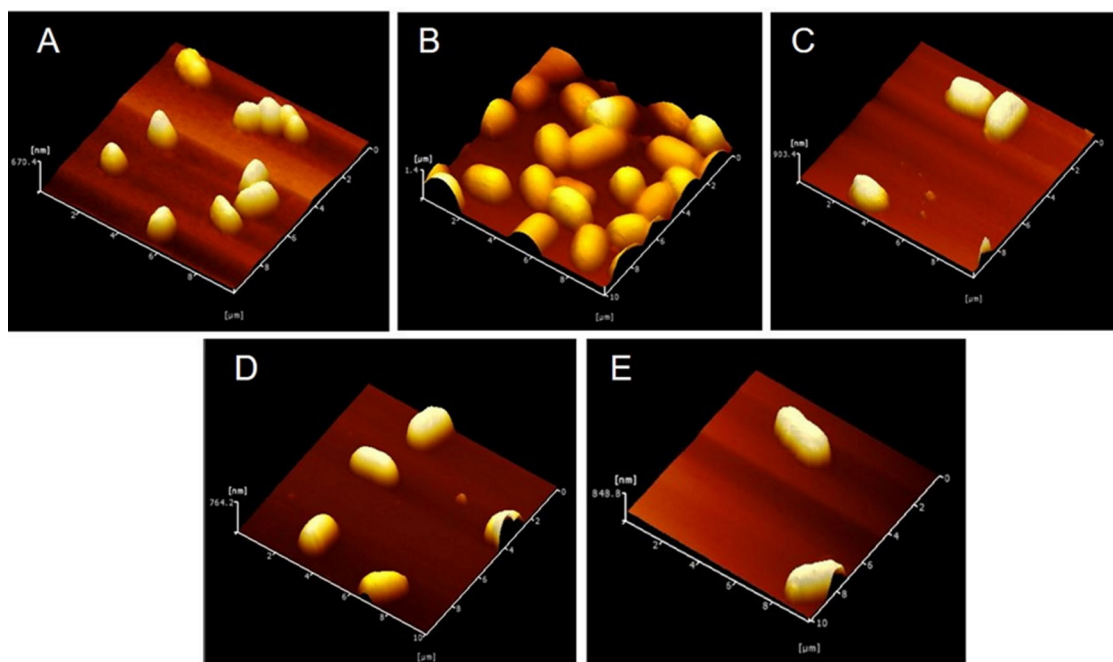


**Figure 1.** Dynamic fluid mode topographical images of *Escherichia coli* ATCC 25404 cells taken under water. The images are 10  $\times$  10  $\mu$ m in size. (A) 3D image of planktonic cells. (B), (C), (D) and (E) are the 3D images of biofilm-dispersed cells from batch cultures by the addition of 0.5, 5, 50  $\mu$ M, and 2.5 mM SNP, respectively.

curve) of the cantilever was obtained and the resonance frequency of the cantilever in water was determined by an atomic force microscope (AFM5100N, Hitachi High-Tech Corp., Tokyo, Japan). Imaging of bacterial cells was initiated with a low scanning speed (0.50 Hz) at a resolution of 256 pixels per line and 256 lines per image using the sampling intelligent scan (SIS) topography method, which is a method based on the dynamic fluid mode (Tapping mode). The SIS mode is an intelligent measurement mode where the scan rate can be freely controlled to match the topography of the sample. In addition, lateral AFM tip-to-sample forces are avoided by the SIS-topography method, as the tip and sample only contact each other when data is required (Hitachi High-Tech Corp.). Images captured by the SIS-topography method were used to locate the cells for force measurements (Figure 1). In addition, the captured images were used to obtain bacterial dimensions (height, width and length values of the cells). Dimensions of the cells were estimated for 18 cells for each investigated using the line-profile section analysis feature of the AFM software and compared using statistical techniques.

When a bacterial cell was located *via* topographical scanning, the oscillation of the cantilever was stopped by switching directly to the contact mode. Pull-off force measurements were then performed in DI water, in which the AFM tip (with a radius of approximately

40 nm) was brought into contact with the bacterial surface and subsequently retracted. At least 25 bacterial cells taken from different cultures were selected for force measurements for each condition investigated. A total of 9–12 points were located on each cell for force measurements using the AFM software, and the retraction force-distance curve between the bacterial surface biopolymers and the silicon nitride AFM tip was measured at each point (Figure 2). Force measurements were also performed on a bacteria-free area of the mica disk before and after measuring a bacterial cell to ensure that the tip was free of contamination from the medium or the sample. Retraction curves obtained from force measurements without any signs of tip-contamination were used in the analyses. Retraction curves were measured at a resolution of 1024 points and analysed to obtain bacterial adhesion forces.

#### Analysis and modelling of retraction curves

At the point where the AFM tip comes into contact with the bacterial surface during a force measurement, the sticky polymers on the bacterial surface adhere to the AFM tip. Then, they break off from the tip when the tip is retracted from the bacterial surface. Since bacterial cell surfaces are known to be composed of a wide variety of surface biopolymers (Moradali and Rehm 2020), it is almost inevitable to

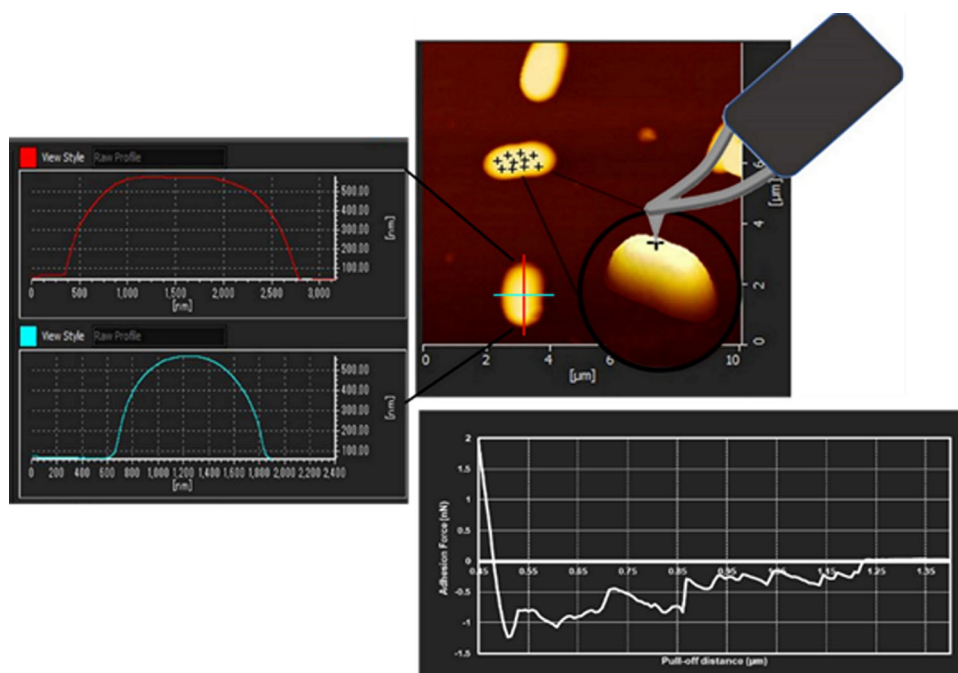


**Figure 2.** Representative figure showing the line-profile section analysis and the force measurement on a bacterial cell. The + signs located on the bacterial surface represent the regions on which the force measurements were performed. A retraction force-distance curve (shown on the right side) was obtained from a single region, and adhesion peaks were determined individually.

observe heterogeneous adhesion events in the retraction curves measured at different spots on a bacterial surface. Due to the heterogeneous nature of the interactions as observed between bacterial surface biopolymers and AFM tips, retraction curves were considered individually and the pull-off force and distance values of the adhesion peaks were evaluated individually using a home-written MATLAB code. Bacterial adhesion strength was reported in terms of adhesion force in nano-Newton (nN) for each investigated (Table 1). In addition, the length of the bacterial surface biopolymers was obtained from their pull-off distances in micro-meter ( $\mu\text{m}$ ), assuming that the molecules were sequentially detached from the tip surface (Arce *et al.* 2004; Deliorman *et al.* 2019). At least 225 retraction curves were examined to evaluate the adhesion forces and pull-off distances for an investigated condition, and at least 856 adhesion peaks were observed among the investigated conditions (Table 1).

To describe the heterogeneities in the adhesion force and pull-off distance data, the mean, median and standard error of the mean values of all adhesion forces and pull-off distances were calculated. In addition, probability histograms of adhesion forces and pull-off distances were generated and the most probable adhesion force and pull-off distance values for each examined condition were determined by

applying log-normal statistical dynamic peak function to the histograms. The log-normal distribution is described as the single-tailed probability distribution of any random variable whose logarithm is normally distributed. The log-normal distribution of the adhesion forces ( $x$ ) is described by:

$$y = \frac{a}{x} \exp \left[ -0.5 \left( \frac{\ln(x/x_0)}{b} \right)^2 \right] \quad (1)$$

where  $y$  is the probability of occurrence of the adhesion (pull-off event),  $x$  is the adhesion tendency,  $a$  and  $b$  are the coefficients of the equation, and  $x_0$  is the parameter expressing the adhesion tendency with the maximum probability of occurrence. Sigma Plot (Systat Software, Inc., Chicago, IL) was used for the estimation of the most probable adhesion force and pull-off distance values for all sets of data.

### Experimental design and statistical analyses

In the first experimental design of this study, SNP concentration was the statistical factor (with 15 levels + 1 control level) whose effect on the biofilm index (response) was determined. A total of 15 different concentrations of SNP were screened for their ability to disperse the pre-formed biofilms. Independent one-way analysis of variance (ANOVA) was

**Table 1.** A summary of the c-di-GMP levels, and the dimensions of planktonic and biofilm-dispersed *Escherichia coli* cells obtained by the addition of media containing different concentrations of SNP, and the most probable values ( $x_0$ ) of nanoscale adhesion forces and lengths (pull-off distances) quantified by fitting lognormal dynamic peak function to the adhesion force, and pull-off distance (PD) data collected between the surface biopolymers of *E. coli* cells and silicon nitride AFM tips under water.

	Planktonic cells	Biofilm-dispersed cells obtained by the addition of SNP			
		0.5 $\mu\text{M}$ SNP	5 $\mu\text{M}$ SNP	50 $\mu\text{M}$ SNP	2.5 mM SNP
c-di-GMP levels of bacterial cells					
pmol c-di-GMP/mg protein	8.4 $\pm$ 0.8	19.6 $\pm$ 3.2	12.8 $\pm$ 0.9	24.2 $\pm$ 0.3	67.3 $\pm$ 0.4
Dimensions of bacterial cells					
Height ( $\mu\text{m}$ )	0.85 $\pm$ 0.08	0.77 $\pm$ 0.22	0.71 $\pm$ 0.26	0.94 $\pm$ 0.23	0.93 $\pm$ 0.28
Width ( $\mu\text{m}$ )	1.10 $\pm$ 0.11	1.94 $\pm$ 0.53	1.17 $\pm$ 0.09	1.32 $\pm$ 0.20	2.16 $\pm$ 0.58
Length ( $\mu\text{m}$ )	1.82 $\pm$ 0.27	3.80 $\pm$ 0.95	2.02 $\pm$ 0.23	2.4 $\pm$ 0.37	3.87 $\pm$ 1.18
Nanoscale adhesion forces of bacterial surface biopolymers					
$x_0$ (nN)	0.279	0.590	0.287	0.492	0.812
$r^2$	0.998	0.996	0.988	0.991	0.978
Mean (nN)	0.347	0.799	0.358	0.594	0.917
SEM (nN)	0.008	0.019	0.011	0.011	0.017
Median (nN)	0.233	0.526	0.220	0.436	0.720
# of adh peaks	1702	1615	856	2760	1974
# of cells	25	25	25	35	25
Lengths (AFM pull-off distances) of bacterial surface biopolymers					
$x_0$ ( $\mu\text{m}$ )	0.638	1.075	0.428	0.578	0.392
$r^2$	0.851	0.991	0.998	0.999	0.999
Mean ( $\mu\text{m}$ )	0.620	1.110	0.496	0.629	0.456
SEM ( $\mu\text{m}$ )	0.008	0.009	0.011	0.005	0.005
Median ( $\mu\text{m}$ )	0.592	1.064	0.433	0.573	0.408
# of PD peaks	1702	1615	856	2760	1974
# of cells	25	25	25	35	25

Lognormal fitting quality ( $r^2$ ) values, and the mean, median, and the standard error of the mean (SEM) of all the data shown in the probability histograms are also given in Table 1.



conducted to determine the SNP concentrations at which the biofilm indexes were significantly lower than that of the control. The second design included factor levels as 0.5, 5, 50  $\mu\text{M}$ , and 2.5 mM of SNP added to pre-formed biofilm cultures to obtain the dispersed cells. In addition, the planktonic cells examined as the control group represented the factor level of 0  $\mu\text{M}$  of added SNP concentration. The response variables investigated were (1) c-di-GMP levels, (2) cellular dimensions, (3) measured nanoscale adhesion forces and (4) lengths of bacterial surface biopolymers. Independent one-way ANOVA was conducted to determine if significant differences in the response variables were present among the planktonic and biofilm-dispersed *E. coli* cells investigated. In addition, Kruskal–Wallis one-way analysis of variance on ranks, the non-parametric equivalent of the one-way ANOVA, and Dunn's pairwise comparison test was performed when required. Sigma Plot (Systat Software, Inc., Chicago, IL) was used for the statistical comparisons of the data sets.

## Results and discussion

### Effect of added SNP concentration on the dispersion of *E. coli* biofilms grown in batch systems

The effect of different doses of NO-donor, SNP, on biofilm dispersion was tested on *E. coli* biofilms grown in batch systems. After 24-h of incubation in SNP-added media, a significant reduction in the biofilm index was observed for those exposed to low doses (in the micromolar range) and 2.5 mM of SNP (Figure 3). Biofilm indexes quantified for low doses of SNP were not statistically different from each other, but on average 70% lower than the biofilm index quantified for the control ( $p < 0.005$ ). In comparison, the biofilm index quantified for 2.5 mM of SNP was 24% lower than the biofilm index quantified for the control ( $p < 0.05$ ), indicating that biofilm dispersion was also induced in media containing 2.5 mM of SNP (Figure 3). In addition, the enumeration of viable bacteria within the biofilms and the microplate wells confirmed the dispersion of biofilms exposed to 0.5, 5, 50  $\mu\text{M}$  and 2.5 mM of SNP concentrations. As fewer bacteria were observed in the biofilms and a greater number of bacteria within the bulk-liquid in the wells for those exposed to SNP treatment compared to those observed for the control (Figure S1).

The biofilm dispersal effect of SNP was previously linked to the release of nitric oxide (NO), which was shown to regulate c-di-GMP levels and mediate *P.*

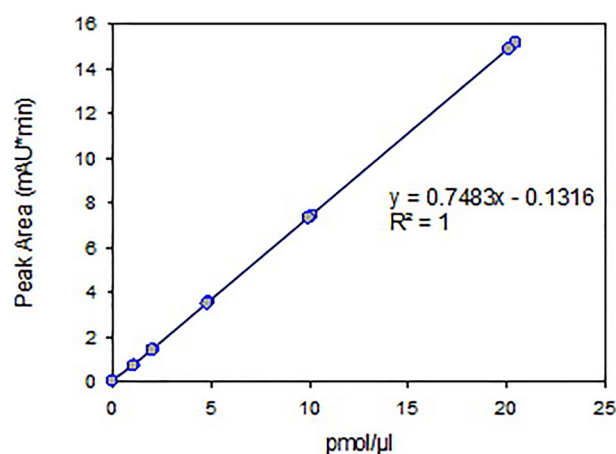


**Figure 3.** Comparison of the mean biofilm indexes of *Escherichia coli* biofilms exposed to different added SNP concentrations for 24-h at 37 °C. Biofilm index was quantified as the ratio of CV staining of the remaining biofilm measured at 595 nm (CV595 nm) to the optical density of the bacterial culture in the well measured at 600 nm (OD600 nm). The control (untreated biofilm, no SNP addition) is given in the figure with an asterisk. (\*\* $p < 0.05$  versus control, \*\*\* $p < 0.005$  versus control).

*aeruginosa* biofilm dispersion when applied at low concentrations (Barraud *et al.* 2006; Chua *et al.* 2014). Other common NO-donors such as S-nitrosoglutathione (GSNO) and S-nitroso-N-acetylpenicillamine (SNAP), were also shown to reduce *P. aeruginosa* biofilm formation. Among them, SNAP was shown to significantly increase the number of dispersed cells while reducing biofilm formation. However, it was reported that SNP was more effective than GSNO and SNAP (Barraud *et al.* 2006; Barraud *et al.* 2009b). In other studies, NO-donors such as 6-(2-hydroxy-1-methyl-2-nitrosohydrazino)-N-methyl-1-hexanamine (MAHMA NONOate), 1-(hydroxy-NNO-azoxy)-L-proline, disodium salt (PROLI NONOate), and spermine NONOate were reported to exhibit higher performances against biofilms (Barnes *et al.* 2013; Barnes *et al.* 2015; Zhu *et al.* 2018). However, besides the performance of the NO-donor, its stability is also an important factor in practice. The use of SNP has the advantage of releasing steady-state levels of NO that mimic endogenous NO production. To characterise NO release from SNP, Bradley and Steinert (2015) recorded NO levels for three consecutive days using NO-sensitive microsensors. They reported that plateau concentrations of NO released from 100  $\mu\text{M}$  SNP in PBS were 70 nM on the first day, 61 nM on the second day, and 64 nM on the third day. Likewise, 200  $\mu\text{M}$  and 300  $\mu\text{M}$  SNP released NO at steady-state and at a concentration approximately 1000-times

lower than the SNP concentration. Barraud *et al.* (2009b) also reported a 1000-fold linear relationship between SNP concentrations (250  $\mu\text{M}$ , 500  $\mu\text{M}$  and 1 mM SNP in PBS) and steady-state levels of NO. Although NO release profiles at very low SNP concentrations (such as 0.5  $\mu\text{M}$  or 5  $\mu\text{M}$  SNP) were not examined in these studies, it can be said that SNP has great stability in releasing consistent NO levels and its concentration has a direct effect on the level of NO released.

As can be seen from Figure 3, biofilm indexes substantially increased at high added SNP concentrations. Previously, Barraud *et al.* (2006) investigated *P. aeruginosa* biofilm growth for 24-h in 96-well plates at 37 °C in the presence of SNP in the range of 25 nM to 100 mM and reported a decrease in biofilm biomass at low SNP concentrations and an increase in biofilm biomass at high millimolar SNP concentrations. As observed for *E. coli* biofilms in this study, and previously for *P. aeruginosa* biofilms, the increase in the biofilm index or the biofilm biomass at high added SNP concentrations might have been related to the adaptation response of the biofilm cells to probably toxic levels of NO and other reactive nitrogen species (RNS) which could have induced extreme nitrosative stress in the cells. NO-mediated toxicity has generally been attributed to the presence of RNS in the medium such as nitrogen dioxide ( $\text{NO}_2$ ) and dinitrogen trioxide ( $\text{N}_2\text{O}_3$ ) (Brunelli *et al.* 1995; Thomas *et al.* 2008), which generate from the reaction of NO with oxygen ( $\text{O}_2$ ) or superoxide ( $\text{O}_2^-$ ). At high concentrations of NO, when the flux of NO exceeds  $\text{O}_2$ ,  $\text{NO}_2$  and  $\text{N}_2\text{O}_3$  are predominantly formed (Thomas *et al.* 2008). In addition, NO could accomplish its toxic effects through reactions with  $\text{O}_2^-$  yielding the potent oxidant, peroxynitrite ( $\text{ONOO}^-$ ) (Brunelli *et al.* 1995; Thomas *et al.* 2008). At low NO fluxes, these reactions would tend to lead to the oxidation of the substrate, while at higher levels of NO they will preferentially nitrosate (Thomas *et al.* 2008). Therefore, the increased biofilm index values at high added SNP concentrations might have been associated with increased EPS productions by the biofilms as a response to the nitrosative stress mediated by high levels of NO and other RNS such as  $\text{NO}_2$  and  $\text{N}_2\text{O}_3$ . Future studies investigating the viable cell counts as well as the amounts of EPS covering the biofilms at high added SNP concentrations may confirm the proposed relationship between increased biofilm indexes and increased EPS productions. Consequently, to investigate the effect of added SNP concentration on the c-di-GMP levels, morphologies, and adhesion

characteristics of biofilm-dispersed cells, cells dispersed from the biofilms by the addition of 0.5  $\mu\text{M}$ , 5  $\mu\text{M}$ , 50  $\mu\text{M}$ , and 2.5 mM of SNP were chosen. In addition to viable cell counts given in Figure S1, fluorescence and AFM images showed that these cells were alive and intact with correct morphology (Figures S4 and 1, respectively).

#### Effect of added SNP concentration on the c-di-GMP levels of planktonic and biofilm-dispersed *E. coli* cells

The c-di-GMP levels of planktonic and biofilm-dispersed cells were found to be statistically and significantly different from each other ( $p < 0.05$ ). As can be seen from Table 1, the lowest c-di-GMP level (8.4 pmol/mg) was detected for the planktonic *E. coli* cells. The level of c-di-GMP in the planktonic *E. coli* cells reported in the present study is consistent with the recently reported level of c-di-GMP in avian pathogenic *E. coli* cells (Liu *et al.* 2021). On the other hand, the highest c-di-GMP level was observed for the cells dispersed by the addition of 2.5 mM of SNP (67.3 pmol c-di-GMP/mg protein), followed by those observed for the cells dispersed by 50, 0.5, and 5  $\mu\text{M}$  added SNP, respectively. In comparison, the c-di-GMP level of the biofilm-dispersed cells obtained by the addition of 5  $\mu\text{M}$  SNP was only 1.5-fold higher than the c-di-GMP level of planktonic cells. However, the c-di-GMP level of the biofilm-dispersed cells obtained by 2.5 mM added SNP was approximately 8-fold higher than that of the planktonic cells (Table 1).

The intracellular level of c-di-GMP is controlled by diguanylate cyclases (DGCs) which synthesize c-di-GMP, and phosphodiesterases (PDEs) which degrade c-di-GMP. In general, biofilm cells and biofilm formation are characterized by a high level of c-di-GMP, which promotes the production of adhesins and matrix components, whereas the presence of NO can activate the phosphodiesterases (PDEs), which hydrolyze c-di-GMP and decrease its intracellular level in biofilm cells and trigger biofilm dispersion (Römling *et al.* 2013; Barraud *et al.* 2015). The correlation between high c-di-GMP level in the cell and biofilm formation or low c-di-GMP level and motility has been demonstrated in several bacterial species, including *E. coli* and *P. aeruginosa* (Simm *et al.* 2004). In *E. coli* K-12, the NO-sensitive repressor protein NsrR was found to be a negative regulator of motility genes and flagella-based motility (Partridge *et al.* 2009). However, it is not clear if NsrR is linked to c-di-GMP or whether it operates *via* an independent pathway in

*E. coli* (Barraud *et al.* 2015). Studies investigating the c-di-GMP levels of planktonic and biofilm-dispersed *P. aeruginosa* cells by the use of SNP were also previously reported in the literature. For example, Chua *et al.* (2014) reported that dispersed cells generated by exposing *P. aeruginosa* biofilms grown in batch cultures to 5  $\mu\text{M}$  SNP for 5-h had a lower c-di-GMP level than their planktonic counterparts. However, Wille *et al.* (2020) reported that dispersed *P. aeruginosa* cells from biofilms cultivated in flow-cells by the sudden addition of 500  $\mu\text{M}$  of SNP had a higher c-di-GMP level than their planktonic counterparts (in comparison, SNP-dispersed cells contained 102.75 nmol c-di-GMP/ $10^6$  CFU, and planktonic cells contained 72.40 nmol c-di-GMP/ $10^6$  CFU). The different results reported for the same bacterial strain (Roy *et al.* 2012; Chua *et al.* 2014; Wille *et al.* 2020) could have resulted from different biofilm cultivation methods and/or different concentrations of SNP used to disperse the biofilms, as observed in the present study.

It is known that diverse stress conditions can induce the general stress response in *E. coli* which controls the expression of signalling enzymes that produce or degrade the c-di-GMP (Pesavento *et al.* 2008; Povolotsky and Hengge 2012). The resulting RNS through the decomposition of SNP in the medium can increase the NO-associated stress responses, as studies of *E. coli* have shown that RNS activate global regulatory networks such as the SOS response (Lobysheva *et al.* 1999; Barraud *et al.* 2006). Hence the observed high levels of c-di-GMP in the biofilm-dispersed cells could have been also related to the adaptive responses of cells exposed to different concentrations of released NO, or specifically to nitrosative stress in the cells due to overproduction of NO and RNS, especially by the addition of 2.5 mM of SNP. Given that at low NO fluxes, reactions would tend to lead to the oxidation of the substrate (Thomas *et al.* 2008), and assuming that a low level of NO was released at steady-state when 0.5  $\mu\text{M}$  of SNP was added to the biofilm culture; the observed high level of c-di-GMP for the cells dispersed by 0.5  $\mu\text{M}$  of added SNP in comparison to that of planktonic cells (Table 1) could have been related to a phenomenon known as oxidative stress, which could have been induced by the presence of oxidants such as ONOO $^-$ . However, a balance can be formed between nitrosative and oxidative chemistry depending on the relative concentration of NO in the medium (Thomas *et al.* 2008). Among the investigated biofilm-dispersed cells, the lowest c-di-

GMP level was observed for cells dispersed by the addition of 5  $\mu\text{M}$  of SNP, suggesting that a threshold level of NO is required to increase oxidative and nitrosative stress responses. Further studies detailing the link between NO and c-di-GMP in planktonic and biofilm-dispersed *E. coli* cells, and investigating the NO release profiles of low dose SNP as well as the concentrations of NO inducing oxidative and nitrosative stress responses may elucidate the observed differences in the c-di-GMP levels of *E. coli* cells dispersed by the addition of different SNP concentrations.

#### **Effect of added SNP concentration on the morphologies of planktonic and biofilm-dispersed *E. coli* cells**

Using the topographic images of bacteria taken by AFM in water (Figure 1), dimensions of planktonic and biofilm-dispersed *E. coli* cells as a function of the added SNP concentration were measured using the AFM software and compared to each other (Figure 4). Pairwise multiple comparison procedure indicated that there were no significant differences among the height values of the bacterial cells examined (Figure 4A). As can also be seen from the similar box plot ranges in Figure 4B and C, the widths and lengths of planktonic cells and dispersed cells obtained by the addition of 5  $\mu\text{M}$  SNP were not significantly different from each other, whereas the widths and lengths of the dispersed cells obtained by 50  $\mu\text{M}$  added SNP were found to be statistically different ( $p=0.021$ ) and on average 16% higher than those of planktonic cells. Similarly, the widths and lengths of the dispersed cells from biofilms by the addition of 0.5  $\mu\text{M}$  and 2.5 mM of SNP were not different from each other, but statistically different ( $p<0.001$ ) and significantly higher than the widths and lengths of other cells investigated (on average 86% wider, and 111% longer than the planktonic cells).

Previously, Kim and Harshey (2016) reported that diguanylate cyclase (DGC) YfiN protein associated with intracellular c-di-GMP production acts as a division inhibitor in response to cell-envelope stress in *E. coli*. After the cell expands to divide, it was shown that YfiN settles in the localization area of division proteins and arrests the division process, and the inhibition of the assembly of division proteins causes an increase in bacterial cell size (Weart *et al.* 2007). In addition, it was also reported that high intracellular c-di-GMP levels are

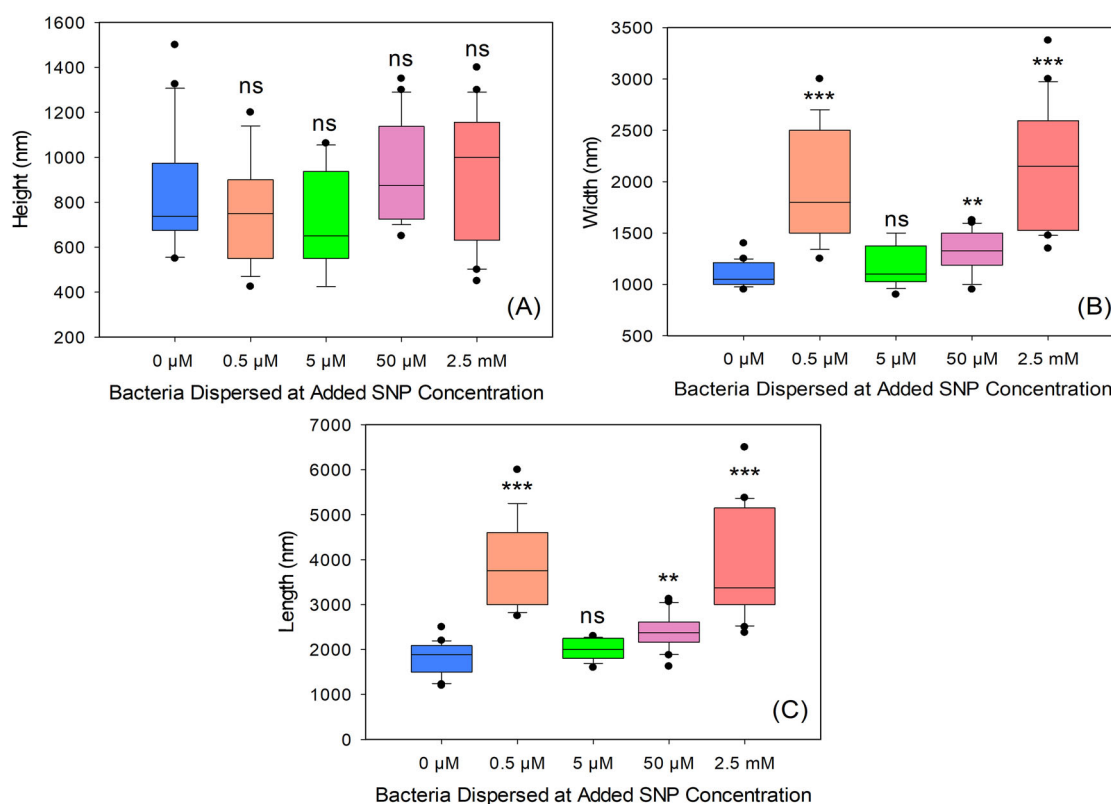


**Figure 4.** Box plots of (A) height, (B) width, and (C) length of planktonic and biofilm-dispersed *Escherichia coli* cells obtained at different added SNP concentrations. Black points indicate 5th/95th percentile outliers. 0 μM of added SNP concentration refers to the planktonic cells, and 0.5, 5, 50 μM and 2.5 mM of added SNP concentrations refer to the cells dispersed from biofilms by the addition of respective SNP concentrations. (ns: not significantly different versus planktonic cells, \*\* $p < 0.05$  versus planktonic cells, \*\*\* $p < 0.001$  versus planktonic cells).

required for mid-cell localization of YfiN in *E. coli*. Likewise, Schäper *et al.* (2016) reported that high *c*-di-GMP levels provoked *Sinorhizobium meliloti* cell elongation, and the highest *c*-di-GMP content resulted in the strongest cell elongation. Since the presence of SNP in the medium results in the formation of NO and other RNS which can lead to an increase in the intracellular *c*-di-GMP level and a possible disruption of the cell envelope by inducing oxidative and/or nitrosative stresses, the observed increase in the length and width of the dispersed cells compared to those of planktonic cells might have been related to the level of their *c*-di-GMP content together with the degree of envelope stress experienced by the cells.

#### Effect of added SNP concentration on the adhesion characteristics of planktonic and biofilm-dispersed *E. coli* cells

##### Nanoscale adhesion forces of bacterial surface biopolymers

As can be seen from Figure 5A–E, the nanoscale adhesion forces measured between the surface

biopolymers of planktonic and biofilm-dispersed *E. coli* cells and silicon nitride AFM tips in water were highly heterogeneous. Statistical comparisons indicated that adhesion forces measured for the planktonic cells and biofilm-dispersed cells obtained by the addition of 5 μM SNP were not significantly different from each other, as can also be seen from their similar distributions given in Figure 5A and C, which were the least heterogeneous among all the adhesion forces presented in Figure 5. However, adhesion forces measured for the other conditions investigated were statistically and significantly different from each other ( $p < 0.001$ ). When compared, the widest distribution of the adhesion forces or the highest heterogeneity in the adhesion force data was observed for the cells dispersed by 2.5 mM and 0.5 μM added SNP concentrations, as evident from the larger span of their adhesion forces (Figure 5B and E), followed by those observed for cells dispersed by 50 and 5 μM added SNP, respectively (Figure 5D and C). To describe the heterogeneity in the distribution of adhesion forces, lognormal dynamic peak function was applied to the probability histograms, and the most probable values of adhesion forces were determined.

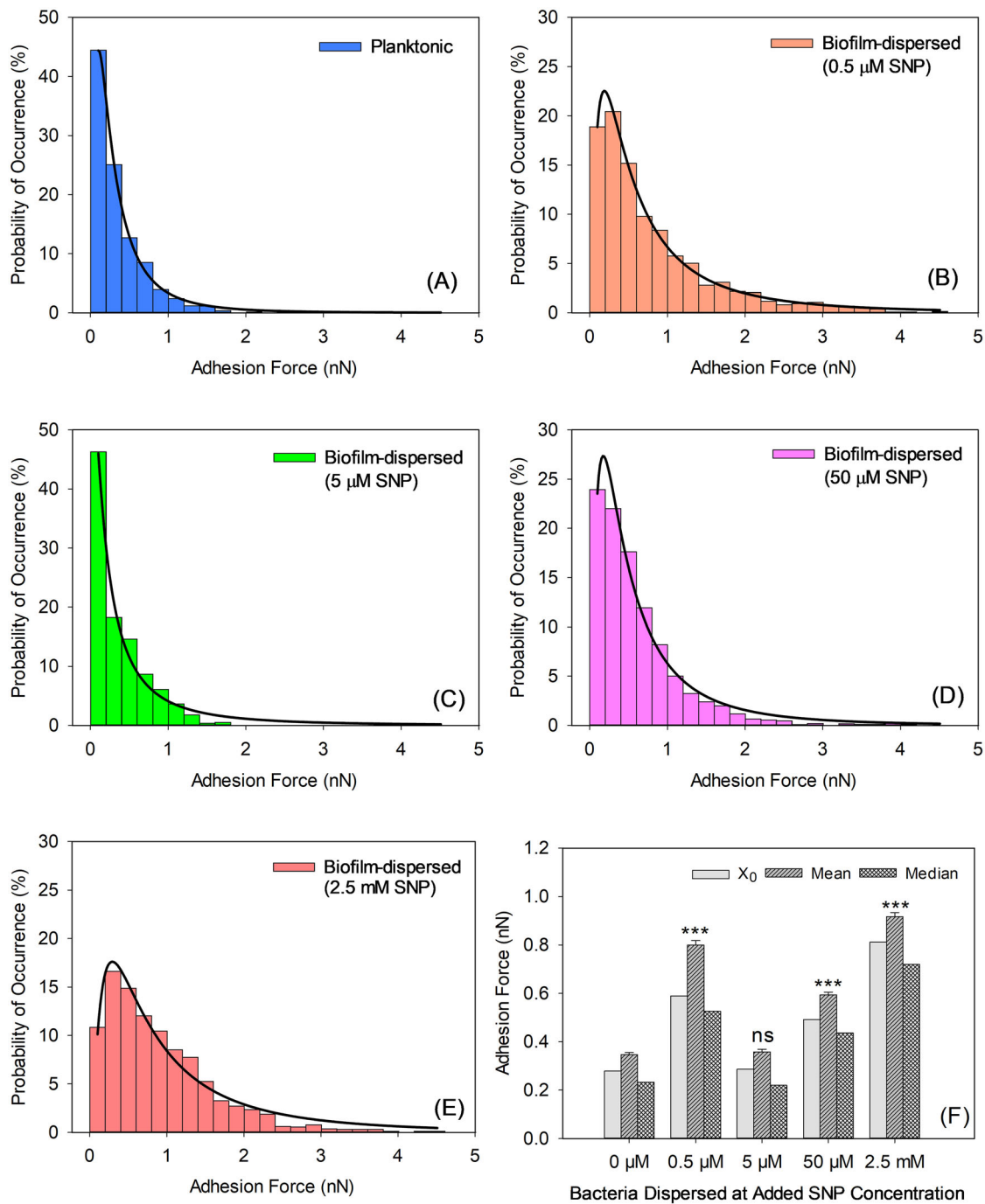


**Figure 5.** (A–E) Histograms showing the distribution of adhesion forces (nN) of *Escherichia coli* cells. Straight lines in histograms indicate that lognormal probability function fits the adhesion force values. (F) Comparison of the most probable, mean and median values of the adhesion forces quantified for planktonic and biofilm-dispersed *E. coli* cells at different added SNP concentrations. 0 μM of SNP concentration refers to the planktonic cells, and 0.5, 5, 50 μM and 2.5 mM of SNP concentrations refer to the cells dispersed from biofilms by the addition of respective SNP concentrations. Error bars represent the standard error of the mean values. (ns: not significantly different versus planktonic cells, \*\*\* $p < 0.001$  versus planktonic cells).

Higher heterogeneity observed in the adhesion force data resulted in higher adhesion strength. The most probable adhesion force obtained for cells dispersed by 2.5 mM added SNP was found to be (0.812 nN) much higher than those obtained for cells dispersed from the biofilms when 0.5, 50 and 5 μM of SNP was

added to the batch cultures of biofilms, respectively (Table 1). The most probable values of adhesion forces obtained for planktonic cells (0.279 nN) and cells dispersed by 5 μM added SNP (0.287 nN) were very close to each other (Table 1), as statistical comparisons showed that the adhesion forces measured

for this pair were not significantly different from each other. The mean and median values of the adhesion forces shown in the distributions were also compared (Table 1, Figure 5F). The mean of the adhesion forces was found to be on average 25% and 33% higher than the most probable and the median adhesion force values, respectively. However, similar trends were observed for the most probable, mean, and median values of the adhesion forces given in the distributions (Figure 5F).

Heterogeneities in AFM data have been largely attributed to the amounts of a wide array of molecules present on the bacterial surface (Dorobantu *et al.* 2008; Ma *et al.* 2008; Park and Abu-Lail 2011). This is because the value of each adhesion force measured by AFM represents an adhesion event between the AFM tip and a biopolymer and/or a group of molecules on the bacterial surface, hence the probability that the AFM tip encounters a different adhesive surface moiety with each adhesion event will be more likely for cells whose surfaces are covered with a higher variety and/or density of adhesive biopolymers (Gordesli-Duatepe *et al.* 2020). In addition, heterogeneities in AFM data can also arise from the phenotypic heterogeneity among a cell population investigated (El-Kirat-Chatel *et al.* 2017), which is a common hallmark of biofilm-dispersed cells (Woo *et al.* 2012; Rumbaugh and Sauer 2020). Considering that c-di-GMP also involves in cell surface remodelling (Jenal 2004; Lacey *et al.* 2010), and the synthesis of various adhesion factors such as curli fimbriae (Hu *et al.* 2013), poly- $\beta$ -1,6-N-acetylglucosamine (Lacanna *et al.* 2016), lipopolysaccharide (McCarthy *et al.* 2017), and several outer membrane proteins (Römling *et al.* 2013), the differences in the nanoscale adhesion strengths of the bacterial cells resulting from the differences in the heterogeneities of their adhesive surface biopolymers could also be dependent on the c-di-GMP levels of the cells. Decoupling of the obtained adhesion forces into specific and non-specific components by the Poisson analysis of the AFM data (Gordesli and Abu-Lail 2012b) can shed light on the contributions of the specific bacterial surface biopolymers to the overall adhesion characteristics of the bacterial cells. In this way, the relationship between the c-di-GMP levels of the cells and the specific adhesion characteristics of their surface biopolymers can be better explained.

The literature lacks information about the nanoscale adhesion characteristics of biofilm-dispersed cells in comparison to their planktonic counterparts regardless of the cultivation method or the dispersion agent/method used. However, colonization and

biofilm-forming abilities of the cells dispersed from biofilms either spontaneously or in response to glutamate have been previously reported in the literature. For example, confocal microscopy observations showed that spontaneously dispersed *K. pneumoniae* cells colonized both abiotic and biotic surfaces more efficiently than their planktonic counterparts (Guilhen *et al.* 2019). Similarly, CV staining confirmed that the biomass on the surfaces of 96-well microplates formed by biofilm-dispersed *P. aeruginosa* cells by the sudden addition of L-glutamate was higher than that of the planktonic cells (Chambers *et al.* 2017). These findings support the results of the present study in that biofilm-dispersed bacterial cells have a higher adhesion capacity than their planktonic counterparts. However, the results of the present study also indicated that the adhesion strengths of the dispersed cells were dependent on the concentration of the dispersing-agent used and the level of intracellular c-di-GMP. As similar levels of c-di-GMP were observed for the planktonic cells and cells dispersed by the addition of 5  $\mu$ M SNP resulted in similar adhesion strengths for this pair. On the other hand, increased c-di-GMP levels enhanced the initial adhesion strength of the bacterial cells (Table 1).

#### Lengths (pull-off distances) of bacterial surface biopolymers

The distributions of the pull-off distances measured between the surface biopolymers of planktonic and biofilm-dispersed *E. coli* cells and silicon nitride AFM tips in water can be seen in Figure 6A–E. The pull-off distance is the separation distance at which the biopolymer attached to the AFM tip is separated from it during retraction. Although the actual lengths of the surface biopolymers of bacterial cells might be longer or shorter, the pull-off distance values could be used as indicators of the lengths of the surface biopolymers of the bacterial cells (Abu-Lail and Camesano 2003). In this context, heterogeneous AFM pull-off distance data (Figure 6A–E) may also indicate the coexistence of various lengths of adhesive surface biopolymers on bacterial surfaces.

Statistical comparisons indicated that pull-off distance values for the cells dispersed by 5  $\mu$ M and 2.5 mM added SNP were not significantly different from each other (Figure 6C and E). However, significant differences were observed between the other pairs examined ( $p < 0.05$ ). As can be seen from Figure 6F, a transition in the pull-off distance values was observed for cells dispersed by 0.5  $\mu$ M added SNP in comparison to other conditions investigated. The

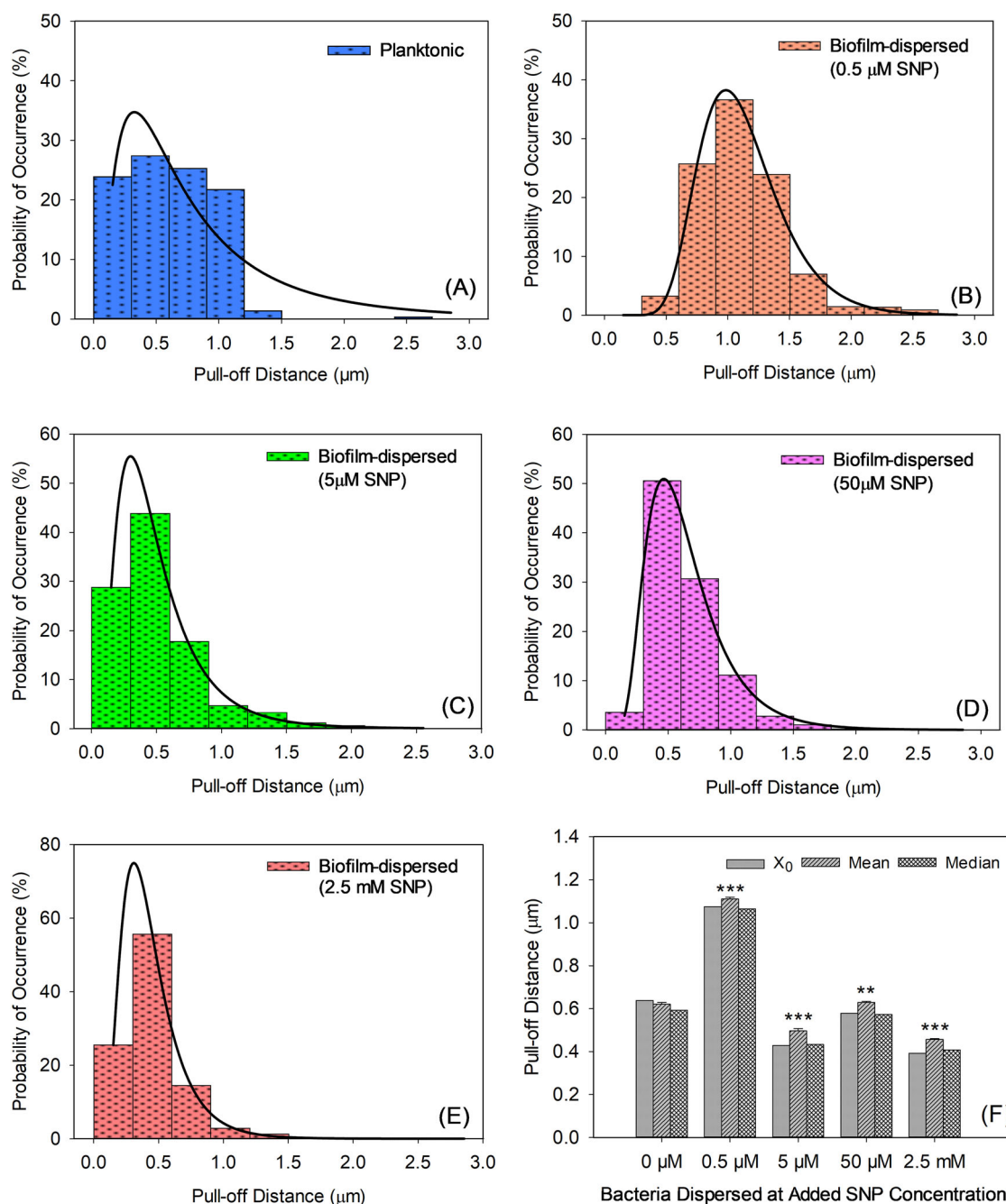


**Figure 6.** (A–E) Histograms showing the distribution of pull-off distances ( $\mu\text{m}$ ) of *Escherichia coli* cells. Straight lines in histograms indicate that lognormal probability function fits the pull-off distance data. (F) Comparison of the most probable, mean and median values of the pull-off distances quantified for planktonic and biofilm-dispersed *E. coli* cells at different added SNP concentrations. 0  $\mu\text{M}$  of SNP concentration refers to the planktonic cells, and 0.5, 5, 50  $\mu\text{M}$  and 2.5 mM of SNP concentrations refer to the cells dispersed from biofilms by the addition of respective SNP concentrations. Error bars represent the standard error of the mean values. (\*\* $p < 0.05$  versus planktonic cells, \*\*\* $p < 0.001$  versus planktonic cells).

most probable pull-off distance obtained for the cells dispersed by the addition of 0.5  $\mu\text{M}$  SNP (1.075  $\mu\text{m}$ ) was found to be much higher than those for planktonic cells and biofilm-dispersed cells obtained by the addition of 50, 5  $\mu\text{M}$ , and 2.5 mM added SNP concentrations, respectively (Table 1). The trends of the most probable, mean, and median values of pull-off

distances were also very similar to each other (Figure 6F). The difference between the mean and the most probable values were on average 8%. In addition, the difference between the median and the most probable values was only 2% on average.

Previous studies showed that the mechanical properties of bacterial surface biopolymers such as the

length and the grafting density were effective in the bacterial adhesion to surfaces. As the length of the surface biopolymers of *E. coli* increased, the strength of bacterial adhesion increased as well (Abu-Lail and Camesano 2003). As in the case of *Listeria monocytogenes*, longer and denser bacterial surface biopolymers were correlated with higher bacterial adhesion strength (Gordesli and Abu-Lail 2012a). In addition, increased adhesion strengths measured by AFM were shown to be inconsistent with the increased lengths of bacterial pili. For the case of *Acinetobacter Venetianus* RAG-1, the adhesion forces extended up to 620 nm from the cell surface, consistent with the lengths of the pili as observed from transmission electron micrographs (Dorobantu *et al.* 2008). Here, the bacteria dispersed by 0.5  $\mu$ M added SNP were found to have longer surface biopolymers than other cells investigated, which might have additionally contributed to their high adhesion strength to silicon nitride surface in water (Table 1, Figure 6F). Although the adhesion strength measured for the cells dispersed by 2.5 mM added SNP was the highest, the length of their surface biopolymers was the shortest, as indicated by the lowest pull-off distance values measured for this group (Table 1). This could be related to the toxic effect of high SNP concentration which might have resulted in collapsed biopolymers (not extended) with a high grafting density on the bacterial surface. Modelling AFM approach curves by steric models that can predict the actual lengths and grafting densities of bacterial surface biopolymers could explain the observed differences in the pull-off distances.

## Conclusions

Induction of biofilm dispersion by NO-donor SNP application has been proposed as a promising strategy for removing biofilms from surfaces due to the safety, stability and efficacy of SNP when applied at low concentrations. The results of this study showed that the addition of 0.5, 5, 50  $\mu$ M and 2.5 mM of SNP to batch cultures of pre-formed *E. coli* biofilms significantly induced dispersion of biofilms. Among the SNP concentrations studied in batch cultures, the optimum concentration of SNP to disperse *E. coli* biofilms was 5  $\mu$ M of SNP, whose addition to batch cultures resulted in the dispersed cells having c-di-GMP levels, morphologies and adhesion strengths similar to their planktonic counterparts. However, dispersed cells obtained by adding other SNP concentrations studied were more adherent and morphologically different than their planktonic counterparts. As indicated from

the results of this study; given the possibility that dispersed cells may have enhanced adhesion characteristics compared to the planktonic cells, depending on the dose of NO-donor applied, the concentration of the NO-donor should be optimized for use in removing biofilms from surfaces.

## Acknowledgements

We would like to thank Prof. Dr. Thomas K. Wood, Biotechnology Endowed Chair and Professor of Chemical Engineering at the Pennsylvania State University, for providing us with the *E. coli* ATCC 25404; and Dr. Colin Grant, former HITACHI SPM Product Manager (Europe), for helping us solve the technical problems we faced when operating the AFM in a liquid environment.

## Disclosure statement

The authors report there are no competing interests to declare.

## Funding

This work was financially supported by The Scientific and Technological Research Council of Turkey (TUBITAK) under TUBITAK 3501-Career Development Grant (Project No: 118M404).

## ORCID

Ayse Ordek  <http://orcid.org/0000-0001-9744-4385>  
F. Pinar Gordesli-Duatepe  <http://orcid.org/0000-0001-8129-6533>

## References

- Abu-Lail NI, Camesano TA. 2003. Role of lipopolysaccharides in the adhesion, retention, and transport of *Escherichia coli* JM109. *Environ Sci Technol.* 37: 2173–2183. doi:10.1021/es026159o
- Arce FT, Avci R, Beech IB, Cooksey KE, Wigglesworth-Cooksey B. 2004. A live bioprobe for studying diatom-surface interactions. *Biophys J.* 87:4284–4297. doi:10.1529/biophysj.104.043307
- Auer GK, Weibel DB. 2017. Bacterial cell mechanics. *Biochemistry.* 56:3710–3724. doi:10.1021/acs.biochem.7b00346
- Alsteens D, Gaub HE, Newton R, Pfreundschuh M, Gerber C, Müller DJ. 2017. Atomic force microscopy-based characterization and design of biointerfaces. *Nat Rev Mater.* 2:17008.
- Barnes RJ, Bandi RR, Wong WS, Barraud N, McDougald D, Fane A, Kjelleberg S, Rice SA. 2013. Optimal dosing regimen of nitric oxide donor compounds for the reduction of *Pseudomonas aeruginosa* biofilm and isolates from wastewater membranes. *Biofouling.* 29:203–212. doi:10.1080/08927014.2012.760069



- Barnes RJ, Low JH, Bandi RR, Tay M, Chua F, Aung T, Fane AG, Kjelleberg S, Rice SA. 2015. Nitric oxide treatment for the control of reverse osmosis membrane biofouling. *Appl Environ Microbiol.* 81:2515–2524. doi:10.1128/AEM.03404-14
- Barraud N, Hassett DJ, Hwang S-H, Rice SA, Kjelleberg S, Webb JS. 2006. Involvement of nitric oxide in biofilm dispersal of *Pseudomonas aeruginosa*. *J Bacteriol.* 188:7344–7353. doi:10.1128/JB.00779-06
- Barraud N, Schleheck D, Klebensberger J, Webb JS, Hassett DJ, Rice SA, Kjelleberg S. 2009a. Nitric oxide signaling in *Pseudomonas aeruginosa* biofilms mediates phosphodiesterase activity, decreased cyclic di-GMP levels, and enhanced dispersal. *J Bacteriol.* 191:7333–7342. doi:10.1128/JB.00975-09
- Barraud N, Storey MV, Moore ZP, Webb JS, Rice SA, Kjelleberg S. 2009b. Nitric oxide-mediated dispersal in single- and multi-species biofilms of clinically and industrially relevant microorganisms. *Microb Biotechnol.* 2:370–378. doi:10.1111/j.1751-7915.2009.00098.x
- Barraud N, Kelso MJ, Rice SA, Kjelleberg S. 2015. Nitric oxide: a key mediator of biofilm dispersal with applications in infectious diseases. *Curr Pharm Des.* 21:31–42. doi:10.2174/1381612820666140905112822
- Bashiri S, Lucidi M, Visaggio D, Capecchi G, Persichetti L, Cincotti G, Visca P, Capellini G. 2021. Growth phase- and desiccation-dependent *Acinetobacter baumannii* morphology: an atomic force microscopy investigation. *Langmuir.* 37:1110–1119. doi:10.1021/acs.langmuir.0c02980
- Borer B, Tecon R, Or D. 2018. Spatial organization of bacterial populations in response to oxygen and carbon counter-gradients in pore networks. *Nat Commun.* 9:769.
- Bradley SA, Steinert JR. 2015. Characterisation and comparison of temporal release profiles of nitric oxide generating donors. *J Neurosci Methods.* 245:116–124. doi:10.1016/j.jneumeth.2015.02.024
- Bridier A, Briandet R, Thomas V, Dubois-Brissonnet F. 2011. Resistance of bacterial biofilms to disinfectants: a review. *Biofouling.* 27:1017–1032. doi:10.1080/08927014.2011.626899
- Brunelli L, Crow JP, Beckman JS. 1995. The comparative toxicity of nitric oxide and peroxyxynitrite to *Escherichia coli*. *Arch Biochem Biophys.* 316:327–334. doi:10.1006/abbi.1995.1044
- Chambers JR, Cherny KE, Sauer K. 2017. Susceptibility of *Pseudomonas aeruginosa* dispersed cells to antimicrobial agents is dependent on the dispersion cue and class of the antimicrobial agent used. *Antimicrob Agents Chemother.* 61:e00846–17. doi:10.1128/AAC.00846-17
- Chua SL, Liu Y, Yam JKH, Chen Y, Vejborg RM, Tan BGC, Kjelleberg S, Tolker Nielsen T, Givskov M, Yang L. 2014. Dispersed cells represent a distinct stage in the transition from bacterial biofilm to planktonic lifestyles. *Nat Commun.* 5:4462. doi:10.1038/ncomms5462
- Davies D. 2003. Understanding biofilm resistance to antibacterial agents. *Nat Rev Drug Discov.* 2:114–122. doi:10.1038/nrd1008
- Deliorman M, Gordesli Duatepe FP, Davenport EK, Fransson BA, Call DR, Beyenal H, Abu-Lail NI. 2019. Responses of *Acinetobacter baumannii* bound and loose extracellular polymeric substances to hyperosmotic agents combined with or without tobramycin: an atomic force microscopy study. *Langmuir.* 35:9071–9083. doi:10.1021/acs.langmuir.9b01227
- Donlan RM. 2002. Biofilms: microbial life on surfaces. *Emerg Infect Dis.* 8:881–890. doi:10.3201/eid0809.020063
- Dorobantu LS, Bhattacharjee S, Foght JM, Gray MR. 2008. Atomic force microscopy measurement of heterogeneity in bacterial surface hydrophobicity. *Langmuir.* 24:4944–4951. doi:10.1021/la7035295
- Dufrène YF. 2015. Sticky microbes: forces in microbial cell adhesion. *Trends Microbiol.* 23:376–382. doi:10.1016/j.tim.2015.01.011
- El-Kirat-Chatel S, Puymege A, Duong TH, Overtvelt PV, Bressy C, Belec L, Dufrène YF, Molmeret M. 2017. Phenotypic heterogeneity in attachment of marine bacteria toward antifouling copolymers unraveled by AFM. *Front Microbiol.* 8:1399.
- Galié S, García-Gutiérrez C, Miguélez EM, Villar CJ, Lombó F. 2018. Biofilms in the food industry: health aspects and control methods. *Front Microbiol.* 9:898. doi:10.3389/fmicb.2018.00898
- Gordesli FP, Abu-Lail NI. 2012a. The role of growth temperature in the adhesion and mechanics of pathogenic *L monocytogenes*: an AFM study. *Langmuir.* 28:1360–1373. doi:10.1021/la203639k
- Gordesli FP, Abu-Lail NI. 2012b. Combined Poisson and soft-particle DLVO analysis of the specificity of the *L monocytogenes* nanoscale adhesion forces measured at varying temperatures of growth. *Environ Sci Technol.* 46:10089–10098. doi:10.1021/es300653w
- Gordesli FP, Abu-Lail NI. 2012c. Impact of ionic strength of growth on the physicochemical properties, structure, and adhesion of *Listeria monocytogenes* polyelectrolyte brushes to a silicon nitride surface in water. *J Colloid Interface Sci.* 388:257–67267.
- Gordesli-Duatepe FP, Park BJ, Kawas LH, Abu-Lail NI. 2020. Atomic force microscopy investigation of the contributions of *Listeria monocytogenes* cell-wall biomacromolecules to their adherence and mechanics. *J Phys Chem B.* 124:5872–5883. doi:10.1021/acs.jpcc.0c04025
- Guilhen C, Miquel S, Charbonnel N, Joseph L, Carrier G, Forestier C, Balestrino D. 2019. Colonization and immune modulation properties of *Klebsiella pneumoniae* biofilm-dispersed cells. *NPJ Biofilms Microbiomes.* 5:25. doi:10.1038/s41522-019-0098-1
- Hall-Stoodley L, Costerton J, Stoodley P. 2004. Bacterial biofilms: from the natural environment to infectious diseases. *Nat Rev Microbiol.* 2:95–108. doi:10.1038/nrmicro821
- Howlin RP, Cathie K, Hall-Stoodley L, Cornelius V, Duignan C, Allan RN, Fernandez BO, Barraud N, Bruce KD, Jefferies J, et al. 2017. Low dose nitric oxide as targeted anti-biofilm adjunctive therapy to treat chronic *Pseudomonas aeruginosa* infection in cystic fibrosis. *Mol Ther.* 25:2104–2116.
- Hu J, Wang B, Fang X, Means WJ, McCormick RJ, Gomelsky M, Zhu MJ. 2013. c-di-GMP signaling regulates *E coli* O157:H7 adhesion to colonic epithelium. *Vet Microbiol.* 164:344–351. doi:10.1016/j.vetmic.2013.02.023
- Jenal U. 2004. Cyclic di-guanosine-monophosphate comes of age: a novel secondary messenger involved in

- modulating cell surface structures in bacteria? *Curr Opin Microbiol.* 7:185–191. doi:10.1016/j.mib.2004.02.007
- Kim HK, Harshey RM. 2016. A diguanylate cyclase acts as a cell division inhibitor in a two-step response to reductive and envelope stresses. *mBio.* 7:e00822–16. doi:10.1128/mBio.00822-16
- Koo H, Raymond NA, Howlin RP, Stoodley P, Hall-Stoodley L. 2017. Targeting microbial biofilms: current and prospective therapeutic strategies. *Nat Rev Microbiol.* 15:740–755. doi:10.1038/nrmicro.2017.99
- Lacanna E, Bigosch C, Kaever V, Boehm A, Becker A. 2016. Evidence for *Escherichia coli* diguanylate cyclase DgcZ interlinking surface sensing and adhesion via multiple regulatory routes. *J Bacteriol.* 198:2524–2535. doi:10.1128/JB.00320-16
- Lacey MM, Partridge JD, Green J. 2010. *Escherichia coli* K-12 YfgF is an anaerobic cyclic di-GMP phosphodiesterase with roles in cell surface remodelling and the oxidative stress response. *Microbiology (Reading).* 156:2873–2886. doi:10.1099/mic.0.037887-0
- Liu J, Zhang D, Lian S, Gu X, Hou Q, Xia P, Zhu G. 2021. Mechanism of nitrite transporter NirC in motility, biofilm formation, and adhesion of avian pathogenic *Escherichia coli*. *Arch Microbiol.* 203:4221–4231. doi:10.1007/s00203-021-02412-5
- Lobysheva II, Stupakova MV, Mikoyan VD, Vasilieva SV, Vanin AF. 1999. Induction of the SOS DNA repair response in *Escherichia coli* by nitric oxide donating agents: dinitrosyl iron complexes with thiol-containing ligands and S-nitrosothiols. *FEBS Lett.* 454:177–180. doi:10.1016/s0014-5793(99)00777-2
- Ma H, Winslow CJ, Logan BE. 2008. Spectral force analysis using atomic force microscopy reveals the importance of surface heterogeneity in bacterial and colloid adhesion to engineered surfaces. *Colloids Surf B Biointerfaces.* 62:232–237. doi:10.1016/j.colsurfb.2007.10.007
- Mah TF. 2012. Biofilm-specific antibiotic resistance. *Future Microbiol.* 7:1061–1072. doi:10.2217/fmb.12.76
- McCarthy RR, Mazon-Moya MJ, Moscoso JA, Hao Y, Lam JS, Bordi C, Mostowy S, Filloux A. 2017. Cyclic-di-GMP regulates lipopolysaccharide modification and contributes to *Pseudomonas aeruginosa* immune evasion. *Nat Microbiol.* 2:17027. doi:10.1038/nmicrobiol.2017.27
- Merritt JH, Kadouri DE, O'Toole GA. 2005. Growing and analyzing static biofilms. *Curr Protoc Microbiol.* Chapter 1:Unit-1B.1. doi:10.1002/9780471729259.mc01b01s00
- Moradali MF, Rehm BHA. 2020. Bacterial biopolymers: from pathogenesis to advanced materials. *Nat Rev Microbiol.* 18:195–210. doi:10.1038/s41579-019-0313-3
- O'Toole GA. 2011. Microtiter dish biofilm formation assay. *J Vis Exp.* 47:2437.
- Park B-J, Abu-Lail NI. 2010. Variations in the nanomechanical properties of virulent and avirulent *Listeria monocytogenes*. *Soft Matter.* 6:3898–3909. doi:10.1039/b927260g
- Park B-J, Abu-Lail NI. 2011. Atomic force microscopy investigations of heterogeneities in the adhesion energies measured between pathogenic and non-pathogenic *Listeria* species and silicon nitride as they correlate to virulence and adherence. *Biofouling.* 27:543–559. doi:10.1080/08927014.2011.584129
- Partridge JD, Bodenmiller DM, Humphrys MS, Spiro S. 2009. NsrR targets in the *Escherichia coli* genome: new insights into DNA sequence requirements for binding and a role for NsrR in the regulation of motility. *Mol Microbiol.* 73:680–694. doi:10.1111/j.1365-2958.2009.06799.x
- Percival SL, Suleman L, Vuotto C, Donelli G. 2015. Healthcare-associated infections, medical devices and biofilms: risk, tolerance and control. *J Med Microbiol.* 64:323–334. doi:10.1099/jmm.0.000032
- Pesavento C, Becker G, Sommerfeldt N, Possling A, Tschowri N, Mehlis A, Hengge R. 2008. Inverse regulatory coordination of motility and curli-mediated adhesion in *Escherichia coli*. *Genes Dev.* 22:2434–2446. doi:10.1101/gad.475808
- Petrova OE, Sauer K. 2017. High-performance liquid chromatography (HPLC)-based detection and quantitation of cellular c-di-GMP. *Methods Mol Biol.* 1657:33–43. doi:10.1007/978-1-4939-7240-1\_4
- Povolotsky TL, Hengge R. 2012. Life-style' control networks in *Escherichia coli*: signaling by the second messenger c-di-GMP. *J Biotechnol.* 160:10–16. doi:10.1016/j.jbiotec.2011.12.024
- Ramezani S, Ta HX, Muhunthan B, Abu-Lail N. 2018. Abu-Lail NI. Role of ionic strength in the retention and initial attachment of *Pseudomonas putida* to quartz sand. *Biointerphases.* 13:041005. doi:10.1116/1.5027735
- Roy AB, Petrova OE, Sauer K. 2012. The phosphodiesterase DipA (PA5017) is essential for *Pseudomonas aeruginosa* biofilm dispersion. *J Bacteriol.* 194:2904–2915. doi:10.1128/JB.05346-11
- Römling U, Galperin MY, Gomelsky M. 2013. Cyclic di-GMP: the first 25 years of a universal bacterial second messenger. *Microbiol Mol Biol Rev.* 77:1–52. doi:10.1128/MMBR.00043-12
- Rumbaugh KP, Sauer K. 2020. Biofilm dispersion. *Nat Rev Microbiol.* 18:571–586. doi:10.1038/s41579-020-0385-0
- Schäper S, Krol E, Skotnicka D, Kaever V, Hilker R, Søgaard-Andersen L, Becker A. 2016. Cyclic di-GMP regulates multiple cellular functions in the symbiotic *Alphaproteobacterium Sinorhizobium meliloti*. *J Bacteriol.* 198:521–535. doi:10.1128/JB.00795-15
- Sharma D, Misba L, Khan AU. 2019. Antibiotics versus biofilm: an emerging battleground in microbial communities. *Antimicrob Resist Infect Control.* 8:76. doi:10.1186/s13756-019-0533-3
- Simm R, Morr M, Kader A, Nimtz M, Römling U. 2004. GGDEF and EAL domains inversely regulate cyclic di-GMP levels and transition from sessility to motility. *Mol Microbiol.* 53:1123–1134. doi:10.1111/j.1365-2958.2004.04206.x
- Soon RL, Nation RL, Hartley PG, Larson I, Li J. 2009. Atomic force microscopy investigation of the morphology and topography of colistin-heteroresistant *Acinetobacter baumannii* strains as a function of growth phase and in response to colistin treatment. *Antimicrob Agents Chemother.* 53:4979–4986. doi:10.1128/AAC.00497-09
- Thomas DD, Ridnour LA, Isenberg JS, Flores-Santana W, Switzer CH, Donzelli S, Hussain P, Vecoli C, Paolucci N, Ambis S, et al. 2008. The chemical biology of nitric oxide:

- implications in cellular signalling. *Free Rad Biol Med.* 45: 18–31. doi:10.1016/j.freeradbiomed.2008.03.020
- Wang YK, Krasnopeeva E, Lin SY, Bai F, Pilizota T, Lo CJ. 2019. Comparison of *Escherichia coli* surface attachment methods for single-cell microscopy. *Sci Rep.* 9:19418. doi:10.1038/s41598-019-55798-0
- Weart RB, Lee AH, Chien AC, Haeusser DP, Hill NS, Levin PA. 2007. A metabolic sensor governing cell size in bacteria. *Cell.* 130:335–347. doi:10.1016/j.cell.2007.05.043
- Werwinski S, Wharton J, Iglesias-Rodriguez M, Stokes K. 2011. Electrochemical sensing of aerobic marine bacterial biofilms and the influence of nitric oxide attachment control. *MRS Proc.* 1356:805. doi:10.1557/opl.2011.1054
- Wille J, Coenye T. 2020. Biofilm dispersion: the key to biofilm eradication or opening Pandora's box? *Biofilm.* 2: 100027. doi:10.1016/j.bioflm.2020.100027
- Wille J, Teirlinck E, Sass A, Van Nieuwerburgh F, Kaever V, Braeckmans K, Coenye T. 2020. Does the mode of dispersion determine the properties of dispersed *Pseudomonas aeruginosa* biofilm cells? *Int J Antimicrob Agents.* 56:106194. doi:10.1016/j.ijantimicag.2020.106194
- Woo JK, Webb JS, Kirov SM, Kjelleberg S, Rice SA. 2012. Biofilm dispersal cells of a cystic fibrosis *Pseudomonas aeruginosa* isolate exhibit variability in functional traits likely to contribute to persistent infection. *FEMS Immunol Med Microbiol.* 66:251–264. doi:10.1111/j.1574-695X.2012.01006.x
- Wood TK, Barrios AFG, Herzberg M, Lee J. 2006. Motility influences biofilm architecture in *Escherichia coli*. *Appl Microbiol Biotechnol.* 72:361–367.
- Zhu X, Oh HS, Ng YCB, Tang PY, Barraud N, Rice SA. 2018. Nitric oxide-mediated induction of dispersal in *Pseudomonas aeruginosa* biofilms is inhibited by flavohemoglobin production and is enhanced by imidazole. *Antimicrob Agents Chemother.* 62:e01832–e01817. doi:10.1128/AAC.01832-17